Quantum Detection using Magnetic Avalanches in Single-Molecule Magnets

Hao Chen,[1] Rupak Mahapatra,[1] Glenn Agnolet,[1] Michael Nippe,[2] Minjie Lu,[1] Philip
C. Bunting,[3] Tom Melia,[4] Surjeet Rajendran,[5] Giorgio Gratta,[6] and Jeffrey Long[7]

[1]*Department of Physics and Astronomy, Texas A&M University, College Station, TX, 77843*
[2]*Department of Chemistry, Texas A&M University, College Station, TX, 77843*
[3]*Department of Chemistry and Biochemistry, University of California San Diego, La Jolla, California 92093*
[4]*Kavli IPMU (WPI), UTIAS, The University of Tokyo, Kashiwa, Chiba 277-8583, Japan*
[5]*Department of Physics & Astronomy, The Johns Hopkins University, Baltimore, Maryland 21218*
[6]*Physics Department, Stanford University, Stanford, CA, 94305*
[7]*Chemistry Department, University of California, Berkeley, CA, 94720*
(Dated: February 24, 2020)

We report the first experimental demonstration of magnetic avalanches induced by scattering of quanta in single-molecule magnet (SMM) crystals made of Mn12-acetate, establishing the use of SMMs as particle detectors for the first time. While the current setup has an energy threshold in the MeV regime, our results motivate the exploration of a wide variety of SMMs whose properties could achieve 10 meV thresholds. If developed, such detectors could serve as single quantum sensors of infrared photons with high efficiency and low dark count rate, and enable the direct detection of sub-GeV dark matter.

Single quantum sensors that can detect energy depositions as low as ~ 10 meV with high efficiency and low false positive (or dark count) rates are of considerable scientific interest. For example, they can be deployed to count single infrared photons, a technical feat of considerable interest to many fields, including quantum computing. This technology can also be leveraged to detect the scattering or absorption of light dark matter. Recently, it was proposed in [1] that such a single quantum sensor could be realized in single crystals of single-molecule magnets (SMMs).

A large variety of SMM molecules can be arranged in a crystalline lattice via standard crystallization techniques. SMMSs are typically comprised of mono- or polynuclear transition metal or lanthanide ion cores that are stabilized by organic ligands. The magnetic anisotropy is hereby of molecular origin and leads to superparamagnetic properties. SMMs exhibit magnetic bistability [2] as the result of a degenerate magnetic ground state and a barrier to reorientation of the magnetization. However, in the presence of an externally applied magnetic field, Zeeman splitting of m_S (or m_J) breaks this degeneracy of the ground state, leading to molecules in metastable magnetic state at low temperatures. For a given SMM material, the lifetime of this metastable state is dependent on temperature. In many cases, this lifetime can be on the order of several months at cryogenic temperatures and in the picosecond regime at higher temperatures. In [1], it was pointed out that this dramatic temperature dependence can be leveraged to amplify the effects of small, localized energy depositions, leading to observable signatures.

In this scheme (see Figure 1), a set of SMM crystals are first magnetically polarized by an external magnetic field. The field is then reversed, which places the molecular spins in the metastable state. The system is held

at cryogenic temperatures, wherein the metastable state has a lifetime of several months. Localized energy deposition heats up a small part of the crystal. As a result of the increased local temperature, the spins in this hot region rapidly relax to the ground state, releasing their stored Zeeman energy. Hence, neighboring spins are heated, causing them to flip as well, releasing even more stored energy. This results in a magnetic "burning" (or deflagration) of the spins in the crystal, wherein all the spins in the entire crystal flip, producing a magnetic "avalanche" that causes a measurable change in the magnetization of the crystal. The process thus amplifies the effect of the initial energy deposition, fueled by the original Zeeman energy. This magnetic avalanche detector is similar in concept to superheated bubble chamber particle detectors, like the PICO detector [3].

As pointed out in [1], carefully designed detectors using SMMs have the potential to detect energy depositions as small as 10 meV. Due to the metastability of the excited Zeeman state at cryogenic temperatures, such detectors would be able to act as high efficiency, low dark count single photon detectors for infrared photons. As dark matter detectors, they could search for the absorption of meV scale "dark photons" or the scattering of $\sim$ keV - MeV mass dark matter particles. Their sensitivity to localized energy depositions, appropriate for these signals, is an important tool in the suppression of backgrounds caused by electron scattering, whereby the same energy is deposited in larger regions, with a density that is insufficient to trigger the magnetic avalanche. Moreover, through the use of precision magnetometers, it may also be possible to identify the location of the scattering event in a bulk volume, so that surface events can be identified, enabling the demarcation of a low background fiducial volume in the bulk.

In this paper, we report the experimental demonstra-

tion of the central concept proposed in [1] *i.e.* the detection of particles by the magnetic avalanches triggered by their scattering in SMM crystals [4]. This demonstration is distinct from prior work on magnetic avalanches in SMM crystals where such avalanches were ignited by directly heating one side of the crystal, supplying energy via surface acoustic waves, or changing the external magnetic field to directly alter the stability of the metastable state [5, 6]. That is, we demonstrate that SMMs can be used as particle detectors, potentially allowing for their use as single quantum sensors in a wide variety of applications.

Mn12-acetate crystals, in which magnetic avalanches had been previously demonstrated using other trigger mechanisms [5, 6], are used in this work. Mn12-acetate crystals with length between 1 and 3 mm and transverse dimensions between 0.5 and 1 mm were synthesized according to published procedures [7].

Crystals are mounted in $3 \times 3 \times 3$ mm^3 sample holders inside a cryogenic setup schematically shown in Figure 2. There are two crystal holders mounted symmetrically, each with its own Hall sensor, in order to detect particles in one of them while using the other as a control sample. Each holder contains a dozen Mn12-acetate crystals, held in place and heat-sunk using epoxy resin. The crystals, as synthesized, have the longer dimension aligned with the easy axis - the axis along which the crystals can be easily magnetized. Care is taken to roughly align the crystals (Figure 2) in the direction of the external magnetic field, in order to maximize the signal. Sample holders and heat

FIG. 2. Schematic view of the experimental setup. SMM crystals are mounted onto two sample holders connected to the same heat sink, each equipped with an independent Hall sensor. An ^{241}Am α source is placed on the upper sample holder, directly facing the SMM crystals within. SMM crystals inside the lower sample holder are shielded from the source, and they are used as control crystals. The lower crystals (Control) are fully covered by epoxy whereas the bottom of the upper crystals (Source) is exposed to the α source.

sinks are made from oxygen-free, high-conductivity copper for optimal heat conduction and non-magnetic properties. Cooling is provided by linking the sample holders to the 1 K pot of a helium-3 cryostat. The cryogenic Hall sensors are in close proximity (1 mm) to the crystals, but thermally isolated from them. The magnetic signal is thus maximized, without the Joule heating from the Hall sensor warming the crystals. The experiment is operated with the sample holders at ~ 1.8 K, as measured by a silicon diode mounted close to the sample holders.

The cryostat is equipped with a superconducting magnet that can provide a magnetic field up to 40 kG. Appropriate controls are available to scan the magnetic field, ramping up and down at selectable rates. The change in the magnetic field near the Hall sensors, caused by an avalanche in the crystals, can be up to 200 G, given the approximate size of the crystals. The Hall sensors used in this experiment were tested to show good linearity in the field range of 0 - 30 kG and a noise level of up to 20 G, thus sufficient for our purpose.

The ^{241}Am source emits α particles with kinetic energy of 5.486 MeV. Care is applied to insure that the epoxy in the source sample doesn't cover the faces of the crystals that are directly exposed to such particles. In the control sample, the SMM crystals are shielded from the α particles by the copper plate separating the source and the bottom sample holder. We expect particle-triggered avalanches only in the sample holder exposed to the source. The metastable time constant at cryogenic temperatures can be sufficiently high for a meaningful experiment, as verified by the control channel of the experiment. Theoretical estimates also show this time constant can be of the order of a few months [1]. The low activ-
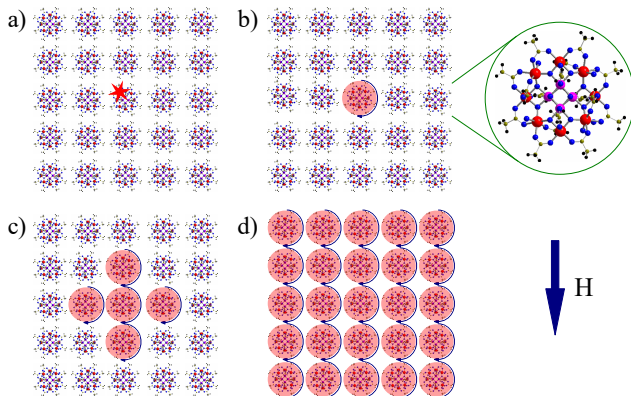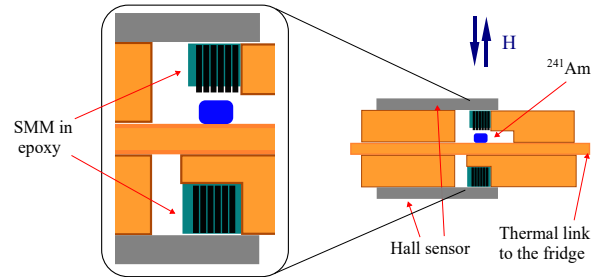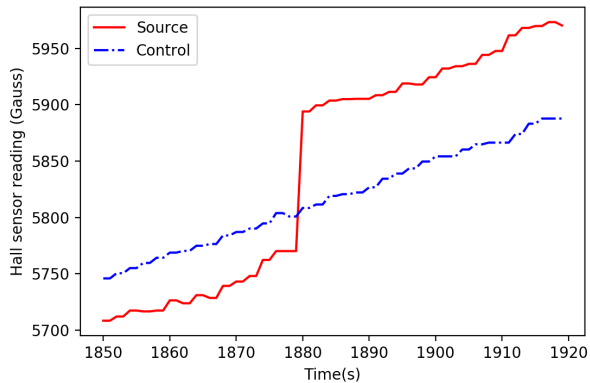

FIG. 1. Conceptual illustration of SMM-based particle detectors. A cryogenic SMM crystal is first polarized at high temperature and the magnetic field is then reversed after cooldown. a) a quatum deposits some energy at a crystal site, b) the deposited energy locally heats the crystal, causing some of the spins to relax, releasing their Zeeman energy, c) the released energy further heats the crystal locally, causing nearby spins to also relax, d) The avalanche process continues until the whole crystal relaxes, with a measurable change in the crystal magnetization.

FIG. 3. Example of an α induced avalanche observed in a reverse field ramp. The change in magnetization is substantially faster than 1 s, characteristic of the expected magnetic avalanche. Note that there is no signal in the control sample at the time of the avalanche. The difference in the calibrated magnetic fields in the Source and the Control Hall sensors is due to the slightly different locations of these 2 samples in the cryostat.
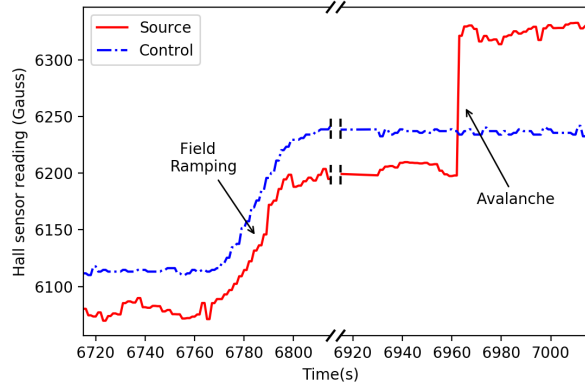

FIG. 4. A particle induced avalanche is observed at constant reverse field, during the scan in small discrete magnetic field steps. Also, in this case, no signal was observed in the control sample at the time of the avalanche. The slow increase in the Hall probe measurements is due to the external field ramp up, whereas the sharp change is due to magnetic avalanche lasting less than a second.

ity α source is expected to produce a low enough rate of less than one per minute to leave substantial time to assess noise in the cryostat that is correlated in the two channels.

The energy threshold required to trigger avalanches in the Mn12-acetate depends on the external magnetic field and is difficult to estimate because some of the parameters of the system are poorly known. Most notably, the thermal conductivity of the crystals in the epoxy is unknown. The threshold is empirically investigated by scanning the external magnetic field both in a continuous mode as well as in discrete steps.

The crystals are initialized by heating them up with a resistor and then ramping up the external field to 10 kG. The field is then either reversed to the desired discrete value or continuously ramped from 0 G to progressively higher reverse values, while monitoring the Hall probes for avalanches. The initialization cycle is repeated at the beginning of each measurement.

In four continuous scans, avalanche events are observed in the crystals exposed to the ^{241}Am source whereas no avalanche is observed in the control ones. The scan rate is of order 2.1 G/s and an example of the observed avalanche is shown in Figure 3. The magnetic field jump is ~ 130 G, consistent with the expectation for Mn12-acetate crystals of the dimensions used here. Avalanches are observed at magnetic fields in the range from 5100 G to 6000 G. In the four scans, the magnetic field jump ranges from 120 G to 140 G.

Similar results are obtained when ramping the magnetic field in discrete steps. In this case, the reverse field is set to constant values and held for 6 to 10 min. If no avalanche signal is observed, the field is then increased by 100 G and held again for each step. This scanning process was repeated seven times, with avalanches observed in 6 of the scans, 5 times while ramping up between the constant field values and once during the constant field. An avalanche at constant field, as observed, is shown in Figure 4. Also in this case, the signal amplitude is slightly larger than 100 G and clearly above the noise level. In each scan, the avalanche was observed only once, implying the entire sample had experienced an avalanche. The magnetic field threshold is around 6000 G, consistent with the value observed for the continuous scans.

During all of the continuous and discrete scans, no magnetic field jump is observed in the control channel and the noise level on either channel is, as shown in the figures, well below the extent of the transitions observed.

In all cases, the magnetic field jumps are abrupt, lasting less than a second and comparable to the ones observed in the literature [8] for SMM triggered by other means and in contrast to the slow ramps of the external field, as shown in Figure 3 and Figure 4. The stability of the SMM system, as observed in the control sample, provides assurance that other sources, such as resonant quantum tunnelling or other magentic relaxation mechanisms do not play a role at these temperatures.

We take this data as clear indication for the observation of magnetic avalanches induced by the absorption of α particles.

This conclusion is corroborated by a few more cross checks. When demagnetizing the samples by increasing their temperatures, the magnetic field change recorded
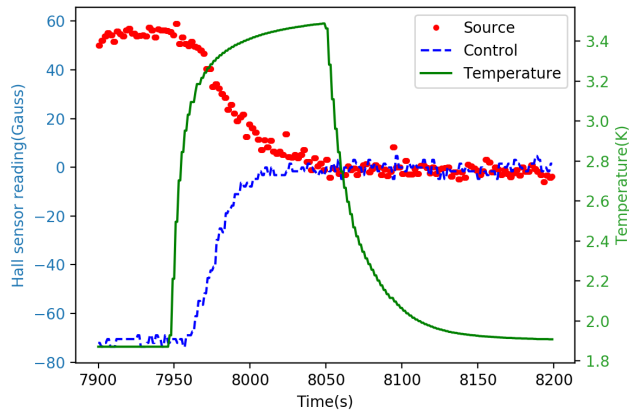
FIG. 5. Demagnetization of Mn12-acetate crystals after an avalanche was observed. The sign for the source and the control sides are opposite, as expected. The amplitude of the transition for the crystals on the source side is 60 G, consistent with half the value measured in an avalanche. The small different in the absolute value of the demagnetization for the source and the control samples is consistent with the uncertainty in the size of the crystals and in the relative positions of the Hall probes.

by the Hall sensors on the two samples are opposite in sign, as shown in Figure 5. This is expected in the case in which the sample exposed to the α particles has reversed magnetization (because the two samples are magnetized by the same field, their initial magnetizations have the same sign). In addition, the Hall sensor reading from the magnetization of the crystal is about 60 G, also shown in Figure 5, which is half the value of the transition in an avalanche. Again, this is expected, because the avalanche reverses the direction of the magnetization.

The probability that the observed transitions are due to some random phenomenon common to the two samples (vibrations, electrical glitches, unstable temperature or background radiation) can be estimated from the control channel and is negligible.

The measurements reported here show that magnetic avalanches in Mn12-acetate SMM crystals can be triggered by the absorption of elementary particles, with a threshold lower than 5.486 MeV for α particles and the values of magnetic field and temperature reported. This demonstrates that SMMs can be used as particle detectors, potentially enabling their application as single quantum sensors in a variety of scientific applications. The predicted and experimentally confirmed energy threshold of Mn12-acetate is comparatively high. The quest for the realization of very low energy detection thresholds motivates future development of SMM materials that display magnetic hysteresis albeit maintaining rather small energy barriers to reorientation of the magnetization. The latter contrasts current trends in SMM research and emphasizes the need for fundamental

research in this area. Furthermore, more measurements with a broader array of SMM materials and similar setups will be required for systematic studies in order to go beyond the current demonstration of the idea put forward in [1].

There is considerable room for exploration. Since their initial discovery [2, 7, 9], many hundreds of new SMMs have been synthesized. While many of them appear to have properties that should allow for the detection of meV-scale energy depositions, not all of their material properties (such as specific heat capacity and thermal conductivity) are known. Before a low threshold detector can be realized, it will be necessary to measure these properties so that an optimal set of SMMs can be identified. Given the promise of SMM detectors and this experimental demonstration, this wider exploration of SMMs with the intent to use them for particle detection is a well motivated enterprise.

———————

[1] P. C. Bunting, G. Gratta, T. Melia, and S. Rajendran, Phys. Rev. D **95**, 095001 (2017).

[2] R. Sessoli, D. Gatteschi, A. Caneschi, and M. A. Novak, Nature **365**, 141 (1993).

[3] C. Amole *et al.* (PICO), Phys. Rev. **D100**, 022001 (2019), arXiv:1902.04031 [astro-ph.CO].

[4] H. Chen, *Magnetic Bubble Chamber Prototype Development*, Ph.D. thesis, Texas A&M Unviersity (2019).

[5] A. Hernández-Mínguez, J. M. Hernandez, F. Macià, A. García-Santiago, J. Tejada, and P. V. Santos, Phys. Rev. Lett. **95**, 217205 (2005).

[6] P. Subedi, S. Vélez, F. Macià, S. Li, M. P. Sarachik, J. Tejada, S. Mukherjee, G. Christou, and A. D. Kent, Phys. Rev. Lett. **110**, 207203 (2013).

[7] T. Lis, Acta Crystallographica Section B **36**, 2042 (1980).

[8] S. McHugh, R. Jaafar, M. P. Sarachik, Y. Myasoedov, A. Finkler, H. Shtrikman, E. Zeldov, R. Bagai, and G. Christou, Phys. Rev. B **76**, 172410 (2007).

[9] A. Caneschi, D. Gatteschi, R. Sessoli, A. L. Barra, L. C. Brunel, and M. Guillot, Journal of the American Chemical Society **113**, 5873 (1991), https://doi.org/10.1021/ja00015a057.